Renewable Energy 39 (2012) 228–240

Contents lists available at SciVerse ScienceDirect

Renewable Energy

journal homepage: www.elsevier.com/locate/renene

Probabilistic approach to multi-objective Volt/Var control of distribution system considering hybrid fuel cell and wind energy sources using Improved Shuffled Frog Leaping Algorithm

Ahmad Reza Malekpour [a,*], Sajad Tabatabaei [b], Taher Niknam [c]

[a] Zarghan Branch, Islamic Azad University, Zarghan, Iran
[b] Department of Electrical Engineering, Mahshahr Branch, Islamic Azad University, Mahshahr, Iran
[c] Marvdasht Branch, Islamic Azad University, Marvdasht, P.O. Box. 73711-13119, Iran

ARTICLE INFO

Article history:
Received 4 December 2010
Accepted 7 August 2011
Available online 3 September 2011

Keywords:
Wind farms
Fuel cell power plant
Stochastic optimization
Volt/Var control
Probabilistic power flow

ABSTRACT

Deregulation and restructuring in power systems, the ever-increasing demand for electricity, and concerns about the environment are the major driving forces for using Renewable Energy Sources (RES). Recently, Wind Farms (WFs) and Fuel Cell Power Plants (FCPPs) have gained great interest by Distribution Companies (DisCos) as the most common RES. In fact, the connection of enormous RES to existing distribution networks has changed the operation of distribution systems. It also affects the Volt/Var control problem, which is one of the most important schemes in distribution networks. Due to the intermittent characteristics of WFs, distribution systems should be analyzed using probabilistic approaches rather than deterministic ones. Therefore, this paper presents a new algorithm for the multi-objective probabilistic Volt/Var control problem in distribution systems including RES. In this regard, a probabilistic load flow based on Point Estimate Method (PEM) is used to consider the effect of uncertainty in electrical power production of WFs as well as load demands. The objective functions, which are investigated here, are the total cost of power generated by WFs, FCPPs and the grid; the total electrical energy losses and the total emission produced by WFs, FCPPs and DisCos. Moreover, a new optimization algorithm based on Improved Shuffled Frog Leaping Algorithm (ISFLA) is proposed to determine the best operating point for the active and reactive power generated by WFs and FCPPs, reactive power values of capacitors, and transformers' tap positions for the next day. Using the fuzzy optimization method and max-min operator, DisCos can find solutions for different objective functions, which are optimal from economical, operational and environmental perspectives. Finally, a practical 85-bus distribution test system is used to investigate the feasibility and effectiveness of the proposed method.

1. Introduction

Uneconomic network expansion to supply remote loads, areas with appropriate capabilities of wind speed and solar radiation [1], environmental concerns about harmful effects of CO_2 emissions, and deregulation and privatization problems are some of the major incentives for the use of clean and sustainable energy resources [2]. Currently, DisCos utilize WFs and FCPPs to generate electric power in a wide range of applications. In fact, in the near future, WFs and FCPPs will be considered as significant sources to generate electric power because of their environmental, social, and economic benefits [1,3].

Challenging issues in distribution systems have emerged due to the wide integration of environmentally friendly energy resources. Moreover, distribution systems usually have radial structures, which include distribution lines with low X/R ratio. Therefore, choosing proper strategies for controlling Volt/Var ratio is of critical importance for DisCos [4]. In this regard, many studies have investigated the daily Volt/Var control problem while the effects of Distributed Generators (DG) are considered in the evaluations [5–14]. In [5–8], the authors have used genetic algorithm and Ant Colony Optimization (ACO) algorithm for optimizing the total active power losses in the Volt/Var control problem. In [9], Niknam has proposed a fuzzy cost-based compensation methodology to solve the daily Volt/Var control problem in distribution networks including DGs. In [10] the problem of voltage rise mitigation in distribution networks considering DGs was studied thoroughly. In [11], minimization of active power losses and micro-generation

* Corresponding author. Tel.: +98 711 7264121; fax: +98 711 7353502.
E-mail addresses: malekpour_ahmad@yahoo.com (A.R. Malekpour), niknam@sutech.ac.ir, taher_nik@yahoo.com (T. Niknam).

0960-1481/$ – see front matter © 2011 Elsevier Ltd. All rights reserved.
doi:10.1016/j.renene.2011.08.004

Nomenclature

List of symbols

$\overline{X}$ state variables vector
N_{DisCo} number of DisCos
N_{WF} number of WFs
N_{FCCP} number of FCPPs
N_t number of transformers
N_c number of capacitors
T number of load variation steps
t index which represents time steps of load level
h^t time interval
$\text{Price}^t_{\text{DisCo},i}$ cost of power supplied by the ith DisCo at the tth hour
$\text{Price}^t_{\text{WF},j}$ cost of power generated by the jth WF at the tth hour
$\text{Price}^t_{\text{FCPP},k}$ cost of power generated by the kth FCPP at the tth hour
$\tilde{P}^t_{\text{DisCo},i}$ expected value of power supplied by the ith DisCo at the tth hour
$\tilde{P}^t_{\text{WF},j}$ expected value of power generated by the jth WF at the tth hour
$\tilde{P}^t_{\text{FCPP},k}$ expected value of power generated by the kth FCPP at the tth hour
$\overline{\text{Tap}}$ tap vector representing tap position of all transformers in the next day
$\overline{\text{Tap}_i}$ tap vector including tap position of the ith transformer in the next day
Tap^t_i tap position of the ith transformer for the tth load level step
$\overline{P_{\text{WF}}}$ WFs active power vector including active power of all WFs in the next day
$\overline{P_{\text{WF}i}}$ WFs active power vector including expected value of active power of the ith WF in the next day
$\tilde{P}^t_{\text{WF}i}$ expected value of active power generated by the ith WF at the tth hour
$\overline{P_{\text{FCPP}}}$ FCPPs active power vector including active power of all FCPPs in the next day
$\overline{P_{\text{FCPP}i}}$ FCPPs active power vector including expected value of active power of the ith FCPP in the next day
$\tilde{P}^t_{\text{FCPP}i}$ expected value of active power generated by the ith FCPP at the tth hour
$\overline{Q_C}$ capacitors reactive power state vector including reactive power of all capacitors in the next day
$\overline{Q_{ci}}$ capacitors reactive power vector including reactive power of ith capacitor in the next day
Q^t_{ci} reactive power of the ith capacitor at the tth hour
N_{br} number of branches
R_i resistance value of the ith branch.
$\tilde{I}^t_i$ expected value of the current for the ith branch at the tth hour
$\tilde{E}^t$ total expected value of emission produced by DisCos, WFs and FCPPs at the tth hour
$\tilde{E}^t_{\text{FC}}$ expected value of emission produced by FCPPs at the tth hour
$\tilde{E}^t_{\text{WF}}$ expected value of emission produced by WFs at the tth hour
$\tilde{E}^{\text{t}}_{\text{DisCo}}$ expected value of emission produced by DisCos at the tth hour
$\text{NO}x^t_{\text{FCPP}}$ nitrogen oxide pollutants of FCPP at the tth hour
$\text{SO2}^t_{\text{FCPP}}$ sulfur oxide pollutants of FCPP at the tth hour
$\text{CO2}^{\text{t}}_{\text{FCPP}}$ carbon dioxide pollutants of FCPP at the tth hour
$\text{NO}x^{\text{t}}_{\text{DisCo}}$ nitrogen oxide pollutants of DisCo at the tth hour
$\text{SO2}^{\text{t}}_{\text{DisCo}}$ sulfur oxide pollutants of DisCo at the tth hour
$\text{CO2}^t_{\text{DisCo}}$ carbon dioxide pollutants of DisCo at the tth hour
P_i net injected active power components at the ith bus
Q_i net injected reactive power components at the ith bus
V_i amplitude of the voltage at the ith bus
δ_i angle of the voltage at the ith bus
Y_{ij} amplitude of the branch admittance between the ith and jth buses
θ_{ij} angle of the branch admittance between the ith and jth buses
$P_{\text{min,FCPP}i}$ minimum active power of the ith FCPP
$Q_{\text{min,FCPP}i}$ minimum reactive power of the ith FCPP
$P_{\text{max,FCPP}i}$ maximum active power of the ith FCPP
$Q_{\text{max,FCPP}i}$ maximum reactive power of the ith FCPP
$P_{\text{min,WF}i}$ minimum active power of the ith WF
$Q_{\text{min,WF}i}$ minimum reactive power of the ith WF
$P_{\text{max,WF}i}$ maximum active power of the ith WF
$Q_{\text{max,WF}i}$ maximum reactive power of the ith WF
$P^{\text{Line}}_{ij,\max}$ maximum active power line flow between the nodes i and j
$|\tilde{P}^{\text{Line}}_{ij}|^t$ expected value of active power line flow between the nodes i and j at the tth hour
$\text{Tap}^{\min}_i$ minimum tap positions of the ith transformer
$Tap^{\max}_i$ maximum tap positions of the ith transformer
Tap^t_i current tap positions of the ith transformer at the tth hour
$Qc^{\min}_i$ minimum reactive power of the ith capacitor
$Qc^{\max}_i$ maximum reactive power of the ith capacitor
Qc^t_i current reactive power of the ith capacitor at the tth hour
$Pf_{\min}$ minimum power factor of DisCo
$Pf_{\max}$ maximum power factor of DisCo
Pf^t current power factor of DisCo at the tth hour
$\tilde{V}^t_i$ expected value of voltage magnitude of the ith bus at the tth hour
$V_{\max}$ maximum value of voltage magnitude
$V_{\min}$ minimum value of voltage magnitude
S probabilistic solution set of output variables
Si ith probabilistic output variable
F set of deterministic power flow equations
z input set of uncertain variables
z_l uncertain input random variable
fz_l probability density function
μ_{Zi} mean value of the input random variable z_i
$Z_{l,1}, Z_{l,2}$ estimated locations of input random variable z_l
$\omega_{l,1}, \omega_{l,2}$ weighting factors for estimated locations of input random variable z_l
m total number of random input variables
$E(S^k_i)$ kth moment of ith output random variable
σ_{zl} standard deviation of z_l
$\lambda_{l,3}$ skewness coefficient of z_l
$\xi_{l,k}$ kth standard location of z_l
μ_{S_i} mean of ith solution random variable
σ_{S_i} standard deviation of ith solution random variable
$f^{\min}_i$ lower limit of ith objective function.
$f^{\max}_i$ upper limit of ith objective function
$f_i(\overline{X})$ ith objective function
$\mu_{f_i}(\overline{X})$ ith membership function
$\text{Object}(\overline{X})$ fuzzy solution multiple objectives
V_i magnitude of voltage at ith bus
δ_i angle of voltage at ith bus
P_g active power of FCPP or WF
Q_g reactive power of FCPP or WF
P_{Load} active power for load

Q_{Load}	reactive power for load
$R + jX$	line impedance
rand()	random number between 0 and 1
D_{min}	minimum permitted variation in frog's position
D_{max}	maximum permitted variation in frog's position
D_i	variation in frog's position
X_{best}	frog with the best fitness
X_{worst}	frog with the worst fitness
X_{global}	global best frog
X_{change}	changing frog position vector
randperm(.)	randomly chosen index from 1,2,…,*n*
P_{WT}	vector of the active power outputs of all wind turbines in all time intervals
P^t_{WT}	active power output of the wind turbine in the tth time interval
$w_{1,2,3,max}$	WT cut-in, rated, cut-off and maximum wind speed, respectively
ψ	a function that converts wind speed to WT power output
$V(I)_{FCPP}$	output voltage (current) of Fuel-Cell
K_P	proportional coefficient
E_0	potential of fuel-cell in thermodynamic equilibrium
w^t	wind speed during hour t
$P_{total\ FCPP}$	total power output of fuel-cell
P_{FCPP}	power output of fuel cell

shedding has been proposed as a methodology to coordinate voltage support in distribution networks with large integration of DGs in micro-grids. The impact of DGs on the existing voltage and reactive power control equipments have been studied in [12]. In [13], Su proposed several voltage control strategies to incorporate existing voltage control devices and reactive power compensators. Senjyu et al. proposed an optimal voltage control scheme considering coordination of DGs, the load ratio control transformers, step voltage regulators, shunt capacitors, shunt reactors, and static Var compensators [14].

According to the recent advances in the wind turbine technology, the utilization of WFs is going to be more popular than before. The stochastic nature of the wind may cause the injection of fluctuated electrical power into the distribution systems [15]. Therefore, extensive study in the field of WF analysis is necessary. Daily load demand is also stochastic due to the heterogeneity of consumers. Hence, Volt/Var control is a complex problem that cannot be solved by deterministic approaches. Deterministic load flow cannot fulfill all the requirements for analyzing a power system with high penetration level of renewable sources of energy. Thus, probabilistic analysis of distribution systems is necessary to cope with all Volt/Var control limitations, which may happen [16]. The Point Estimate Method (PEM) is a reliable and proficient method for modeling uncertainty in the power systems [17]. Consequently, in this paper, PEM has been applied to model the load/generation uncertainty in the Volt/Var control problem.

In some studies, probabilistic load flow is used to consider the effect of wind power plant integration on the voltage control of distribution systems. In [18], the adjustment of voltage regulators and switched capacitors as reactive power control devices in distribution networks was studied based on the probabilistic load flow analysis. The objective functions were the total power losses and the voltage fluctuations. In addition, multi-parameter control strategies were employed to alleviate the violation of constraints. In [19], Hatziargyriou applied a constrained probabilistic load flow to the tap settings as well as the reactive compensation devices simultaneously. In this work, various rates of wind power penetration were considered to show the effectiveness of the methodology.

In [20], a probabilistic load flow was utilized to investigate the voltage fluctuations in the high wind power penetrated systems. Uncertainties caused by the wind speed variations, load fluctuations, generator outages, and branch outages were taken into account. Hong and Luo [21] presented a method based on genetic algorithm using wind generator voltages, static compensators, and transformer taps as controllers to regulate the voltage profile for probabilistic operation planning in the distribution systems. In [22], a new method was proposed to consider the impact of the stochastic behavior of the loads and DG power productions as well as the operation of voltage control devices and random network configuration on the voltage profile in the network.

In all previous studies, the daily Volt/Var control has been modeled as a single-objective optimization problem. Recently, environmental concerns about global warming and greenhouse gases have led to extensive use of emission-free plants such as WFs and FCPPs, which can greatly reduce nitrogen and sulfur oxides emissions. Hence, in this paper, RES are considered in order to reduce the amount of total emission as one of the main objective functions. The total power loss due to the small X/R ratio of distribution lines is considered as another important objective function and its effect on Volt/Var control problem is investigated. Also, the total cost of power generation by WFs, FCPPs, and the distribution companies is taken into account to achieve an economic plan for the Volt/Var control problem.

The main purpose of this article is to develop a multi-objective probabilistic daily Volt/Var control strategy for distribution networks regarding the probabilistic characteristics of wind farms and daily load, operation of voltage control devices, and the deterministic nature of FCPPs. The control variables are the active and reactive power production of WFs and FCPPs, reactive power of capacitors and transformers' tap in the next day. Initially, the objective functions are modeled with fuzzy sets to consider their imprecise nature. Later, the transformers' tap, reactive power of capacitors, bus voltages magnitude as well as the stochastic active and reactive power of WFs and FCPPs are obtained using the max–min operator and probabilistic power flow.

The control devices such as capacitors, DGs, and load tap changers convert the optimal daily Volt/Var control strategy to a mixed integer nonlinear problem. Among different methods to solve these types of problems, the conventional and classical methods may end up in a local minimum rather than a global one and some of them cannot handle the integer problems [5–9]. Consequently, evolutionary algorithms because of their independency from the type of objective functions and constraints, have been used by many researchers in recent years [7–9]. One of the new evolutionary algorithms with a great potential for optimization applications is the Shuffled Frog Leaping Algorithm (SFLA). In fact, this algorithm can solve complex optimization problems, which are nonlinear, non-differentiable and multi-modal but it may trap in local optima. To overcome this problem, in this paper a new SFLA algorithm is proposed to improve the local exploration of the algorithm in the entire search space. The main idea behind the new frog leaping rule is to extend the direction and the length of each frog's jump by emulating the frog's perceptions. The modification expands the local search space and improves the performance of the SFLA.

2. Problem formulation

As mentioned before, power systems are inherently stochastic due to uncertainties in both intermittent energy sources and load demands. Consequently, the bus voltages, the active and reactive

power flows and power losses, the emission generated by DisCos, WFs and FCPPs, and the total cost should be calculated in a probabilistic environment.

It should be noted that superscript ~ indicates the expectation of random variables.

2.1. Decision variables

$$X = [\overline{\text{Tap}}, \overline{P_{\text{WF}}}, \overline{Q_{\text{WF}}}, \overline{P_{\text{FCPP}}}, \overline{Q_{\text{FCPP}}}, \overline{Q_C}]_{1\times n}$$

$$\overline{\text{Tap}} = [\overline{\text{Tap}_1}, \overline{\text{Tap}_2}, \ldots, \overline{\text{Tap}_{Nt}}]_{1\times(T\times Nt)}$$

$$\overline{\text{Tap}_i} = \left[\text{Tap}_i^1, \text{Tap}_i^2, \ldots, \text{Tap}_i^T\right]_{1\times T} \quad \text{i} = 1,2,3,\ldots,N_{\text{t}}$$

$$\overline{P_{\text{WF}}} = [\overline{P_{\text{WF1}}}, \overline{P_{\text{WF2}}}, \ldots, \overline{P_{\text{WF }N\text{WF}}}]_{1\times(T\times N\text{WF})}$$

$$\overline{P_{\text{WF}i}} = \left[\tilde{P}_{\text{WF}i}^1, \tilde{P}_{\text{WF}i}^1, \ldots, \tilde{P}_{\text{WF}i}^T\right]_{1\times T} \quad \text{i} = 1,2,3,\ldots,N\text{WF}$$

$$\overline{Q_{\text{WF}}} = [\overline{Q_{\text{WF1}}}, \overline{Q_{\text{WF2}}}, \ldots, \overline{Q_{\text{WF }N\text{WF}}}]_{1\times(T\times N\text{WF})}$$

$$\overline{Q_{\text{WF}i}} = \left[\tilde{Q}_{\text{WF}i}^1, \tilde{Q}_{\text{WF}i}^2, \ldots, \tilde{Q}_{\text{WF}i}^T\right]_{1\times T} \quad \text{i} = 1,2,3,\ldots,N\text{WF}$$

$$\overline{P_{\text{FCPP}}} = [\overline{P_{\text{FCPP1}}}, \overline{P_{\text{FCPP2}}}, \ldots, \overline{P_{\text{FCPP }N\text{FCPP}i}}]_{1\times(T\times N\text{FCPP})}$$

$$\overline{P_{\text{FCPP}i}} = \left[\tilde{P}_{\text{FCPP}i}^1, \tilde{P}_{\text{FCPP}i}^2, \ldots, \tilde{P}_{\text{FCPP}i}^T\right]_{1\times T} \quad \text{i} = 1,2,3,\ldots,N\text{FCPP}$$

$$\overline{Q_{\text{FCPP}}} = [\overline{Q_{\text{FCPP1}}}, \overline{Q_{\text{FCPP2}}}, \ldots, \overline{Q_{\text{FCPP }N\text{FCPP}i}}]_{1\times(T\times N\text{FCPP})}$$

$$\overline{Q_{\text{FCPP}i}} = \left[\tilde{Q}_{\text{FCPP}i}^1, \tilde{Q}_{\text{FCPP}i}^2, \ldots, \tilde{Q}_{\text{FCPP}i}^T\right]_{1\times T} \quad \text{i} = 1,2,3,\ldots,N\text{FCPP}$$

$$\overline{Q_C} = [\overline{Q_{c1}}, \overline{Q_{c2}}, \ldots, \overline{Q_{cNc}}]_{1\times(T\times Nc)}$$

$$\overline{Q_{ci}} = \left[Q_{ci}^1, Q_{ci}^2, \ldots, Q_{ci}^T\right]_{1\times T} \quad \text{i} = 1,2,3,\ldots,N_{\text{c}}$$

$$n = T\times(N_t + N_{\text{WF}} + N_{\text{FCPP}} + N_c)$$

2.2. Objective functions

The objective functions are defined as follows:

2.2.1. Total electrical energy costs generated by FCPPs, WFs and DisCos

One of the main objective functions in the deregulated power market is the total electrical energy cost.

$$\begin{aligned}\tilde{f}_1(X) &= \sum_{t=1}^{T} C^t\\ C^t &= \sum_{i=1}^{N\text{DisCo}} \text{Price}_{\text{DisCo},i}^t\cdot\tilde{P}_{\text{DisCo},i}^t\cdot h^t + \sum_{j=1}^{N_{\text{WF}}} \text{Price}_{\text{WF},j}^t\cdot\tilde{P}_{\text{WF},j}^t\cdot h^t\\ &\quad + \sum_{k=1}^{N_{\text{FCCP}}} \text{Price}_{\text{FCPP},k}^t\cdot\tilde{P}_{\text{FCPP},k}^t\cdot h^t\end{aligned} \tag{1}$$

Here, it is assumed that the tap position of transformers can change stepwise.

2.2.2. Total electrical energy losses

The total electrical energy for the next day ahead can be defined as follows:

$$\tilde{f}_2(X) = \sum_{t=1}^{T}\sum_{i=1}^{N_{\text{br}}}\left(R_i\cdot|\tilde{I}_i^t|^2\cdot h^t\right) \tag{2}$$

2.2.3. Emission generated by DisCo, WFs, and FCPPs

Emission produced by DisCos, WFs, and FCPP as the third objective function is calculated as follows:

$$\begin{aligned}\min\ \tilde{f}_3(X) &= \sum_{t=1}^{T}\tilde{E}^t = \sum_{t=1}^{T}\left(\tilde{E}_{\text{FC}}^t + \tilde{E}_{\text{WF}}^t + \tilde{E}_{\text{DisCo}}^t\right)\\ \tilde{E}_{\text{FCPP}}^t &= \text{CO}_{2_{\text{FCPP}}}^t + \text{NO}x_{\text{FCPP}}^t + \text{SO}_{2_{\text{FCPP}}}^t\\ &= (1078 + 0.03 + 0.006)^{\text{lb/MWh}}\cdot\sum_{j=1}^{N_{\text{FCPP}}}\tilde{P}_{\text{FCPP}_j}^t\\ \tilde{E}_{\text{DisCo}}^t &= CO_{2_{\text{DisCo}}}^t + NOx_{\text{DisCo}}^t + SO_{2_{\text{DisCo}}}^t\\ &= (2031 + 5.06 + 7.9)^{\text{lb/MWh}}\cdot\tilde{P}_{\text{DisCo}}^t\\ \tilde{E}_{\text{WF}}^t &= 0\end{aligned} \tag{3}$$

where $\tilde{P}_{\text{DisCo}}^t$ is the expected active power infeed to the distribution system at hour t.

2.3. Constraints

In order to have an optimal plan while maintaining the security and operational conditions, the following constraints should be met:

2.3.1. Distribution power flow equations

$$\begin{aligned}P_i &= \sum_{i=1}^{N_{\text{bus}}} V_iV_jY_{ij}\cos\left(\theta_{ij} - \delta_i + \delta_j\right)\\ Q_i &= \sum_{i=1}^{N_{\text{bus}}} V_iV_jY_{ij}\sin\left(\theta_{ij} - \delta_i + \delta_j\right)\end{aligned} \tag{4}$$

2.3.2. Hourly limits on WFs and FCPPs's active power

$$\begin{aligned}P_{\min,\text{FCPP}i} \le \tilde{P}_{\text{FCPP}i}^t \le P_{\max,\text{FCPP}i}\\ P_{\min,\text{WF}i} \le \tilde{P}_{\text{WF}i}^t \le P_{\max,\text{WF}i}\end{aligned} \tag{5}$$

2.3.3. Hourly limits on WFs and FCPPs's reactive power

$$\begin{aligned}Q_{\min,\text{FCPP}i} \le \tilde{Q}_{\text{FCPP}i}^t \le Q_{\max,\text{FCPP}i}\\ Q_{\min,\text{WF}i} \le \tilde{Q}_{\text{WF}i}^t \le Q_{\max,\text{WF}i}\end{aligned} \tag{6}$$

2.3.4. Line flow limits

$$\left|\tilde{P}_{ij}^{\text{Line}}\right|^t < P_{ij,\max}^{\text{Line}} \tag{7}$$

2.3.5. Limits on the transformers' tap

$$\mathrm{Tap}_i^{\min} < \mathrm{Tap}_i^t < \mathrm{Tap}_i^{\max} \tag{8}$$

2.3.6. Hourly limits on capacitors reactive power

$$Qc_i^{\min} < Qc_i^t < Qc_i^{\max} \tag{9}$$

2.3.7. Hourly limits on DisCo power factor

$$Pf_{\min} \le Pf^t \le Pf_{\max} \tag{10}$$

2.3.8. Hourly limits on bus voltage magnitude

$$V_{\min} \le \tilde{V}_i^t \le V_{\max} \tag{11}$$

3. Modeling RES in distribution systems

Different models of RES according to their operation technology and connection to the grid are as follows:

3.1. Wind farms (WFs)

WFs are categorized into two different types of fixed and variable speed units. The first type uses a squirrel cage induction generator and is directly connected to the network through a gear box. The second type uses a synchronous or double-fed induction generator and is connected to the utility grid through power electronic devices. The output power varies with respect to the wind speed. The wind turbine active power is mathematically described by [25]:

$$P_{\mathrm{WT}}^t = \begin{cases} 0 & w^t \le w_1 \text{ or } w^t \ge w_3 \\ \psi(w^t) & w_1 \le w^t \le w_2 \\ P_{\mathrm{WT}} & w_2 \le w^t \le w_3 \end{cases} \qquad t = 1,2,\ldots,T \tag{12}$$

3.2. Fuel cell power plants (FCPPs)

FCPPs are electrochemical plants, which have low emissions with a wide range of applications. Unlike the traditional power generators, they have no rotating part and can convert the chemical energy directly to the electrical power. In fact, power electronics interfaces are employed to connect FCPPs to the utility grid. The FCPP output power can be calculated as follows [26]:

$$P_{\mathrm{FCPP}} = V_{\mathrm{FCPP}} \cdot I_{\mathrm{FCPP}} \tag{13}$$

If the inner resistance of the FCPP is R, the total electrical power, which is converted by this unit is evaluated as follows:

$$P_{\text{total FCPP}} = P_{\mathrm{FCPP}} + R \cdot I_{\mathrm{FCPP}}^2 \tag{14}$$

Here, the regulation of electric power generation of a fuel-cell is defined as:

$$P_{\text{total FCPP}} = K_p \cdot (E_0 - V_{\mathrm{FCPP}})^2 \tag{15}$$

4. The effect of WFs and FCPPs on voltage profile of distribution networks

Investment tax credit and imposition of carbon tax have attracted DisCos' attention to sustainable plants and RES more than before. However, DisCos will face new technical and operational challenges with the proliferation of RES. With installation of WFs and FCPPs in the distribution networks, any change in the power flow may change the voltage profile. Since the X/R ratio of the distribution lines is small, the WF or FCPP has much impact on the voltage profile. To show this influence, consider the 2-bus test system of Fig. 2. The voltage drop along the line from bus 1 to bus 2 is calculated as follows:

$$\begin{aligned} \Delta V &= V_1 \angle \delta_1 - V_2 \angle \delta_2 = (R + jX)I \\ I &= \frac{P - jQ}{V_2^*} \\ P &= P_g + P_{\mathrm{Load}} \\ Q &= Q_g + Q_{\mathrm{Load}} \\ |\Delta V|^2 &= \frac{(RP + XQ)^2 + (XP - RQ)^2}{V_2^2} \approx \frac{(RP + XQ)^2}{V_2^2} \end{aligned} \tag{16}$$

It is obvious from the above equation that neither RP nor XQ is negligible. Also, since the X/R ratio is small and Q is less than P, the impact of the active power of WFs or FCPPs on the system voltage is much more than their reactive power.

5. Probabilistic power flow

Regarding the uncertainty in the power systems especially in load demand and WF output power prediction, it is necessary for power system planners to use stochastic models. Therefore, in this paper, probabilistic power flow based on Point Estimate Method (PEM) is utilized to consider the effects of this uncertainty as much as possible. PEM was first introduced by Rosenblueth [27]. In the original PEM, the number of algorithms, which are required to evaluate a system with n random variables is 2^n. Later, Hong [28] developed an alternative PEM for multivariable system analysis, which reduced the number of computations from 2^n to $2n$. Finally, Morales [24] and Su [29] used Hong's $2n$ point estimate method to implement the probabilistic load flow problem. The deterministic power flow can be expressed mathematically as follows:

$$S = F(z) \tag{17}$$

Indeed, the effect of uncertainties, which exist in the load/generation in the set of input variables (z), will be transformed to the solution set of output variables (S) through the nonlinear power flow function F [30]. In the context of probabilistic load flow, the goal is to find the Probability Distribution Function (PDF) of output variables S based on the statistical information of z.

In the $2n$ PEM approach, every uncertain variable is replaced with only two deterministic points named estimated locations, $Z_{l,1}$, $Z_{l,2}$. The two estimated locations are placed on each side of the corresponding mean value of the PDF. In particular, (13) is decomposed into several sub-problems by considering only two deterministic values for each uncertain variable. Next, the deterministic power flow is run twice for each uncertain variable (i.e. the value below the mean, $Z_{l,2}$, and the value above the mean, $Z_{l,1}$) while the other variables are kept at their mean values, μ_{Z_i}.

$$S = F(\mu_{Z_1}, \mu_{Z_2}, \ldots, Z_{l,k}, \ldots, \mu_{Z_m}) \quad k = 1,2 \tag{18}$$

The $2n$ PEM needs $2n$ runs of deterministic power flow for n uncertain variables. In comparison to Monte Carlo approach [31], this property effectively reduces the computational burden.

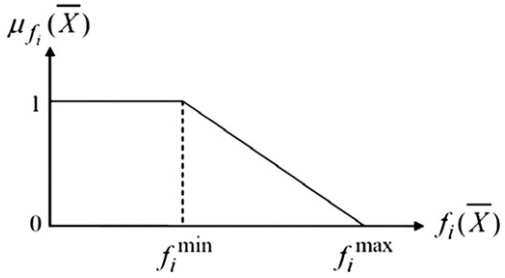

Fig. 1. The membership function for objective functions.

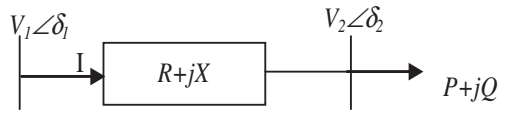

Fig. 2. . 2-bus test system.

The locations $Z_{l,k}$ $(k = 1, 2)$ of the random input variable Z_l are specified values of Z_l, which are calculated from its statistical moments. The only required statistical information are the first three central moments; mean, variance, and coefficient of skewness.

For each solution, when the $2n$ deterministic load flow are calculated, the kth moment of the output random variable can be obtained by multiplying the power of the kth solution by a weighting factor, whose values depend on the statistical moments of the input random variables.

This paper focuses on the uncertainties related to RES and load demands. It is assumed that their statistical features are estimated or measured, and there is no correlation between input random variables including active and reactive power generations and load values.

The procedure to compute the moments of output random variables in the $2m$ point estimate scheme are summarized as:

Step 1: Determining the number of input random variables m.
Step 2: Setting $E(S^1) = 0$, $E(S^2) = 0$
Step 3: Setting $l = 1$.
Step 4: Calculating the skewness coefficient of z_l:

$$\lambda_{l,3} = \frac{E\left[(z_l - \mu_{zl})^3\right]}{(\sigma_{Pl})^3} \tag{19}$$

whereμ_{zl}, σ_{zl}, $\lambda_{l,3}$ are the mean, standard deviation and skewness coefficient of z_l, respectively. Also, E denotes the expectation operator.

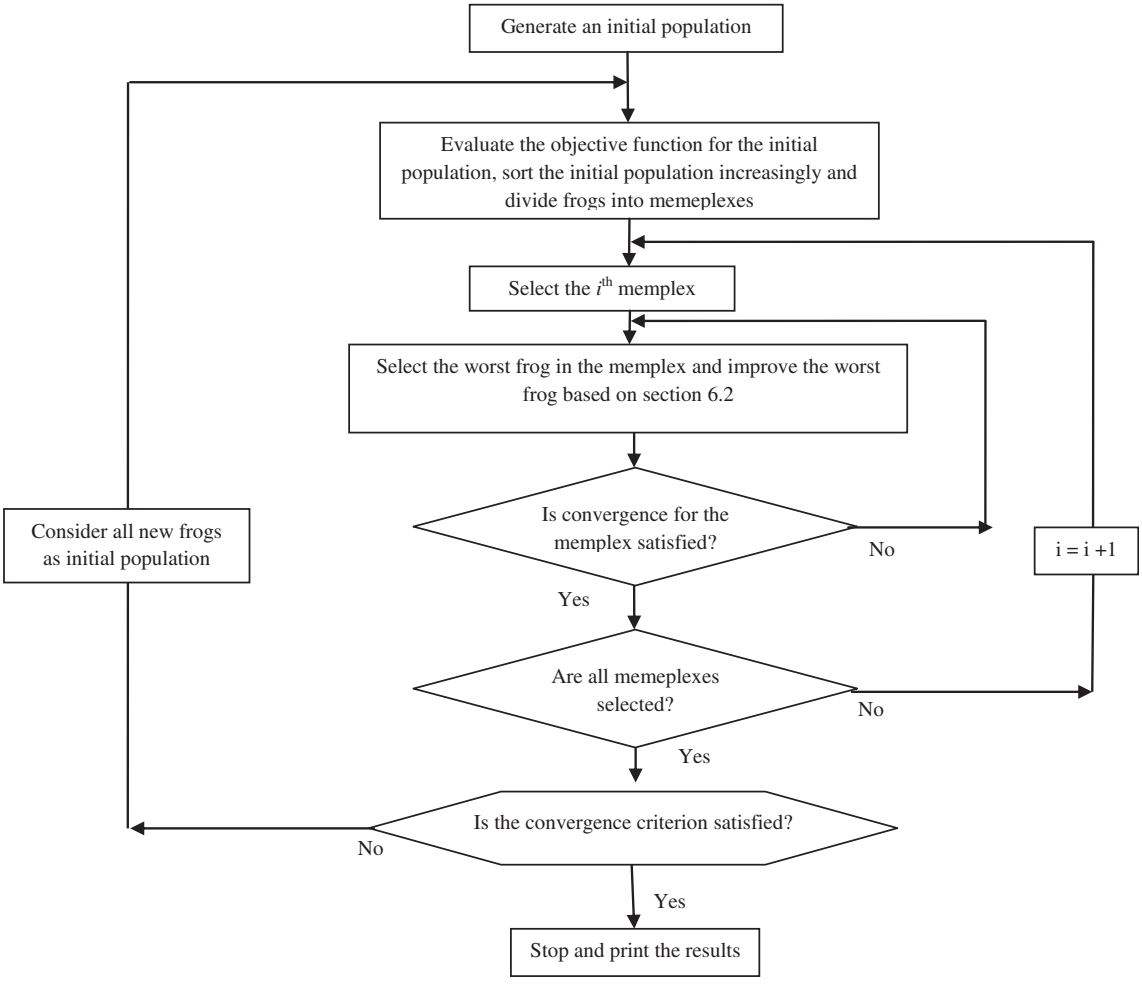

Fig. 3. Flowchart of the ISFLA.

Step 5: Calculating the two standard locations:

$$\xi_{l,1} = \frac{\lambda_{l,3}}{2} + \sqrt{m + \left(\frac{\lambda_{l,3}}{2}\right)^2}\ ,\ \xi_{l,2} = \frac{\lambda_{l,3}}{2} + \sqrt{m + \left(\frac{\lambda_{l,3}}{2}\right)^2} \tag{20}$$

Step 6: Calculating the two estimated locations:

$$z_{l,1} = \mu_{zl} + \xi_{l,1}\cdot\sigma_{zl},\ z_{l,2} = \mu_{zl} + \xi_{l,2}\cdot\sigma_{zl} \tag{21}$$

Step 7: Running deterministic power flow for both estimated locations:

$$\begin{aligned} S_{(l,1)} &= F(\mu_{z_1}, \mu_{z_2}, \ldots, Z_{l,1}, \ldots, \mu_{z_m}) \\ S_{(l,2)} &= F(\mu_{z_1}, \mu_{z_2}, \ldots, Z_{l,2}, \ldots, \mu_{z_m}) \end{aligned} \tag{22}$$

Step 8: Computing the two weighting factors:

$$\omega_{l,1} = -\frac{1}{m}\frac{\xi_{l,2}}{\xi_{l,1} - \xi_{l,2}},\ \omega_{l,2} = -\frac{1}{m}\frac{\xi_{l,1}}{\xi_{l,1} - \xi_{l,2}} \tag{23}$$

Step 9: Updating the first and the second moment of output random variables:

Table 1
Characteristics of installed RESs.

RES type	Capacity (KW)	Location	Power factor
WF_1	500	6	0.9 lag to 0.9 lead
$FCPP_1$	500	12	0.9 lag to 0.9 lead
$FCPP_2$	300	19	0.9 lag to 0.9 lead
$FCPP_3$	300	28	0.9 lag to 0.9 lead
$FCPP_4$	500	31	0.9 lag to 0.9 lead
WF_2	500	71	0.9 lag to 0.9 lead
$FCPP_5$	500	75	0.9 lag to 0.9 lead
WF_3	500	79	0.9 lag to 0.9 lead

$$E\left(S_i^k\right) = E\left(S_i^k\right) + \sum_{k=1}^{2} \omega_{l,k}\cdot S_{i(l,k)} \tag{24}$$

Step 10: Repeating steps 4–9 for $l = l + 1$ until all uncertain parameters are taken into account.
Step 11: Computing mean and standard deviation of solution random variables.

$$\mu_{S_i} = E(S_i),\ \sigma_{S_i} = \sqrt{E\left(S_i^2\right) - (E(S_i))^2} \tag{25}$$

Once mean and standard deviation of solution random variables are known, their probability density functions can be approximated and plotted by Gram-Charlier series approach [32].

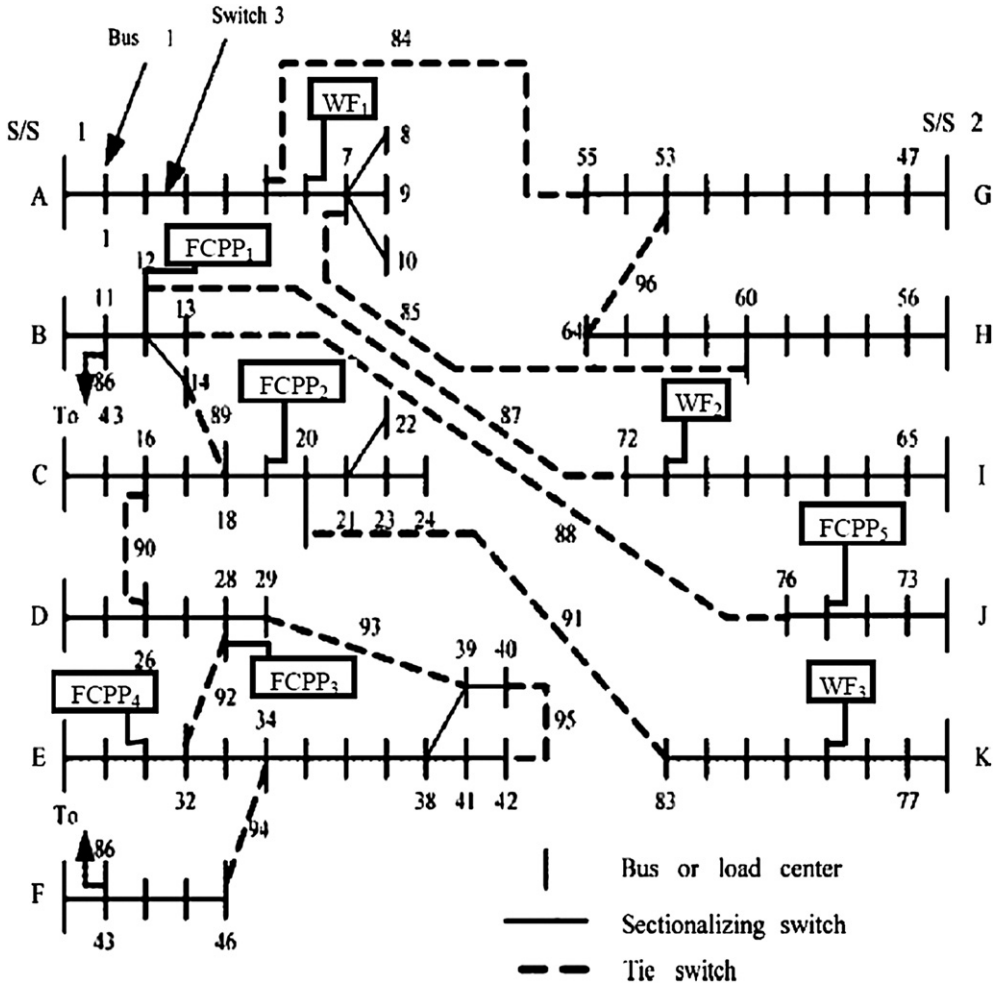

Fig. 4. Single line diagram of 69 bus test system.

6. Fuzzy model for the multi-objective probabilistic daily Volt/Var control

As mentioned before, here a fuzzy optimization algorithm is utilized to solve the multi-objective probabilistic daily Volt/Var control. The objective functions are modeled by membership functions to attain the optimal solution [33]. The membership function for the *i*th objective function has been shown in Fig. 1. The *i*th membership function is defined as follows:

$$\mu_{f_i}(\overline{X}) = \begin{cases} 1 & f_i(\overline{X}) \le f_i^{\min} \\ \dfrac{f_i^{\max} - f_i(\overline{X})}{f_i^{\max} - f_i^{\min}} & f_i^{\min} \le f_i(\overline{X}) \le f_i^{\max} \\ 0 & f_i(\overline{X}) \ge f_i^{\max} \end{cases} \quad (26)$$

where $f_i^{\min}$, $f_i^{\max}$ are evaluated by the single optimization of each objective function, separately.

For multiple objective problems, the fuzzy solution can be calculated as follows:

$$\text{Object}(\overline{X}) = \min\left[\mu_{f1}(\overline{X}), \mu_{f2}(\overline{X}), \mu_{f3}(\overline{X})\right] \quad (27)$$

The maximum value of Object$(\overline{X})$ is considered as the optimal solution.

7. Shuffled Frog Leaping Algorithm (SFLA)

7.1. The basic concept of SFLA

SFLA is a new member of meta-heuristic search algorithms and there are a few papers in the literature to address SFLA. This new algorithm was first introduced by Eusuff and Lansey [34]. Then, Eusuff et al. developed the SFLA to solve the combinatorial optimization problems [35]. Later, SFLA was applied to solve a mixed-model assembly line sequencing problem [36], clustering [37], permutation flow shop scheduling problem [38], and general large-scale water supply system [39]. Also, Elbeltagi et al. compared the formulations and results of five evolutionary-based algorithms, i.e. Genetic Algorithms, Memetic Algorithms, Particle Swarm, Ant-colony systems, and Shuffled Frog Leaping Algorithm [23] to show the ability of SFLA.

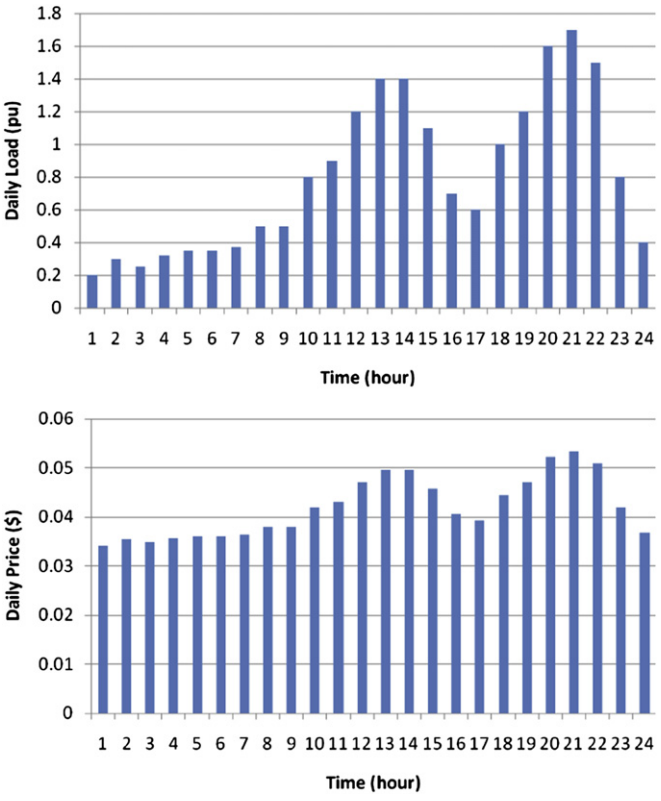

Fig. 5. Daily energy price and load variations.

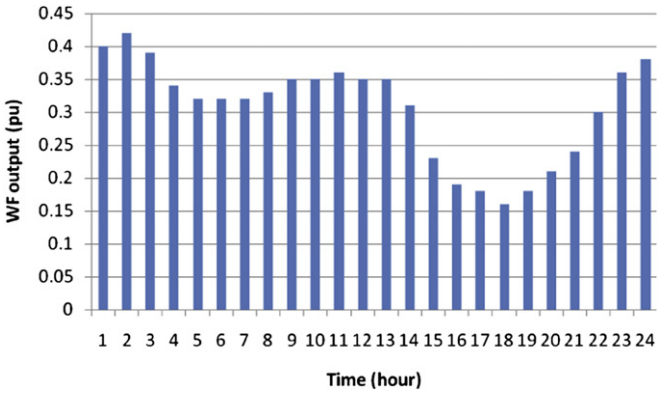

Fig. 6. The hourly active power output of WFs.

SFLA is based on the natural behavior of frogs searching for food. A population of memes, which embody the position of frogs is divided into different subsets called memeplexes. The solution exploration is based on the local search in each memeplex as well as global search in the whole population. Firstly, the local search is performed for a predefined number of iterations. Then, the virtual frogs are shuffled and reorganized into new memeplexes in a technique similar to that in the Shuffled Complex Evolution Algorithm. Moreover, to provide the opportunity for random generation of improved information, random virtual frogs are generated and substituted in the population. The local search and the shuffling process continue until the predefined convergence criteria are satisfied.

In the original SFLA, the position of the frog with the worst fitness is adjusted as follows:

$$\text{Changeing frog position}(D_i) = \text{rand}() \times (X_{\text{best}} - X_{\text{worst}}) \quad (28)$$

$$X_{\text{worst}}^{\text{new}} = X_{\text{worst}}^{\text{old}} + D_i; \quad D_{\min} \le D_i \le D_{\max} \quad (29)$$

where rand(.) is a random number between 0 and 1; and $D_{\min}$ and $D_{\max}$ are the minimum and the maximum permitted variation in the frog's position. If this process produces a better frog, it replaces the worst one; else the calculations in Eqs. (27) and (28) are repeated with respect to the global best frog (i.e. X_{global} replaces

Table 2
Comparison of expected values for average, the best and the worst solutions using the PSO, SFLA and ISFLA methods.

Objective function	Method	Average	Worst solution	Best solution
Emission (Kg)	ISFLA	763412557	808543861	719038033
	SFLA	786423521	834672464	719038033
	PSO	779853216	816493531	719038033
Cost ($)	ISFLA	39752642	42367854	36797825
	SFLA	40982342	45623412	36797825
	PSO	40074376	43917382	36797825
P_{Loss} (Kwh)	ISFLA	16091.5	17381.54	15641.92
	SFLA	16743.1	17989.1	15641.92
	PSO	16094.9	17590.7	15641.92

X_{best}). If no improvement is achieved in the latter case, then, a new solution is randomly generated to replace the worst frog with another one having any arbitrary fitness.

7.2. Improved SFLA algorithm

The original SFLA may be trapped in local optima due to its drawback in finding the worst frog position. In this paper, two new modifications are employed to overcome the aforementioned deficiencies. In each memeplex, the position of the frog with the worst fitness is adjusted as follows:

$$\begin{aligned} \Delta X_{\text{improved1}} &= \text{rand}(.)\cdot(X_{\text{best}} - T_F \cdot X_M) \\ X^{new}_{\text{worst}} &= X^{\text{old}}_{\text{worst}} + \Delta X_{\text{improved1}} \end{aligned} \tag{30}$$

where, X_M is the mean value of individuals in each memeplex. T_F is a heuristically determined constant factor and is chosen randomly from values 1 or 2. (T_F = round [1 + rand(0, 1)]).

To improve the diversity of the search space vector, a frog X_j is selected from the population of the frogs such that$X_j \neq X_i$. Subsequently, the position is determined using the following equation.

$$\begin{aligned} &\textit{if } f(X_j) \geq f(X_i) \\ &\quad \Delta X_{\text{improved2}} = \text{rand}(.)\cdot(X_j - X_i) \\ &\textit{else} \\ &\quad \Delta X_{\text{improved2}} = \text{rand}(.)\cdot(X_i - X_j) \\ &\textit{end} \end{aligned} \tag{31}$$

The new improved individual is generated as follows:

$$X_i^{\text{new}} = X_i^{\text{old}} + \Delta X_{\text{improved2}} \tag{32}$$

If the performance of the generated frogs in Eqs. (29) or (31) is better than the worst frog, it replaces the worst frog. Otherwise a new solution is generated by a Chaotic Local Search (CLS), as follows:

At first, the best solution in each memeplex is considered as an initial solution (X^0_{cls}) for CLS, where X^0_{cls} is scaled into $[0, 1]$ according the following equation:

$$\begin{aligned} X^0_{\text{cls}} &= \left[x^1_{\text{cls},0}, x^2_{\text{cls},0}, \ldots, x^n_{\text{cls},0}\right]_{1\times n} \\ Cx_0 &= \left[cx^1_0, cx^2_0, \ldots, cx^n_0\right] \\ cx^j_0 &= \frac{x^j_{\text{cls},0} - x_{j,\min}}{x_{j,\max} - x_{j,\min}}, j = 1.2, \ldots, n \end{aligned} \tag{33}$$

Then, the chaos population for CLS is generated as:

$$\begin{aligned} X^i_{\text{cls}} &= \left[x^1_{\text{cls},i}, x^2_{\text{cls},i}, \ldots, x^n_{\text{cls},i}\right]_{1\times n}, i = 1, 2, \ldots, N_{\text{choas}} \\ x^j_{\text{cls},i} &= cx^j_{i-1} \times (x_{j,\max} - x_{j,\min}) + x_{j,\min}, j = 1.2, \ldots, n \end{aligned} \tag{34}$$

where, cx^j_i indicates the jth chaotic variable and N_{choas} is the number of individuals for CLS. Then, the best solution among them is replaced with the worst solution. Fig. 3 shows the flowchart of ISFLA algorithm applied to the Volt/Var control problem.

8. Simulation

To demonstrate the effect of uncertainty in WFs and load demands on the daily Volt/Var control problem, the 85-bus distribution test feeder shown in Fig. 4 is used as the case study [40]. The system contains two substations and 11 feeders. The tap position of voltage regulators ranges from 0.95 to 1.05 with a step of 0.01. The installation node and capacity of RES are shown in Table 1. The cost of energy generated by FCPPs and WFs are 0.045, 0.41 ($/MWh), respectively. The installed capacitors are at infeed buses and buses #21, #34, #64 and #83 with their maximum capacities of 600 kVar for infeed buses and 500 kVar for buses #21, #34, #64 and #83 with 100 kVar step change. The daily load and energy price variation are shown in Fig. 5.

Regarding the uncertainty in the load demand, it is assumed that buses #41 and #58 have discrete distribution. Normal distribution with a constant standard deviation of 5% is considered for buses #9, #10, #14, #18, #27, #45, #51 and 83. The other feeder loads are assumed to have deterministic nature (zero standard deviation).

The random output powers of WFs are modeled with Weibull distribution with 5 impulses to calculate the mean and the standard deviation of WFs per hour. The shape and scale parameter of the distribution parameters can be found in [41]. Using the distribution parameters, the hourly active power output of WFs is calculated as shown in Fig. 6.

In order to clearly illustrate the effectiveness of the proposed method, Table 2 provides a complete comparison among the results obtained by ISFLA, SFLA and PSO algorithms for the three objective functions. As shown in Table 2, the smallest and the largest values of the minimized objective function are referred to as the "Best Solution" and the "Worst Solution", respectively. Comparing the best and the worst solutions of the proposed optimization algorithm with those of SFLA and PSO methods, the effectiveness of the proposed method is quite obvious. Moreover, the table provides the average value of the objective functions (minimized) values, based on ISFLA, SFLA and PSO methods. It can be noticed from Table 2 that in the proposed algorithm, the foregoing variables' values are assumed considerably smaller than their corresponding values in SFLA and PSO methods.

Table 3 shows the stochastic daily variation of electrical energy costs, active power losses and emissions for the best solutions during the next day. It can be seen that the energy cost, power

Table 3
Daily expected values of electrical energy costs, active power losses and emissions for the best solutions.

Hour	Cost ($)	P_{Loss} (kW)	Emission (Kg)	Hour	Cost ($)	P_{Loss} (kW)	Emission (Kg)
1	79009.62	5.895081	2033222	13	3677844	1711.083	69008000
2	182665.8	18.58782	4663561	14	3687172	1709.803	69008000
3	127224.7	11.31563	3361824	15	2580174	968.3539	52210000
4	200661.5	21.373	5290933	16	675098.4	171.3804	15432274
5	237994.5	27.71024	6082653	17	541180.7	114.5889	12769003
6	237109.7	27.58124	5961293	18	1217346	419.7722	25402254
7	258007	32.11484	6691981	19	2928514	1197.708	58112000
8	408477	73.3804	10251363	20	4490236	2343.8	80358000
9	409725.1	73.67191	10018141	21	4934294	2706.409	85806000
10	820505.7	228.8824	18119649	22	4084196	2011.792	74456000
11	968103.2	309.548	20827389	23	819826	231.6964	18092264
12	2940409	1186.085	57658000	24	292050.8	39.38623	7424228
Sum Cost = 36797825, Sum P_{Loss} = 15641.92, Sum Emission = 719038033							

Table 4
Expected values of daily optimal dispatches of WFs and FCPPs.

Hour	WF1 (kW)	WF1 (kvar)	WF2 (kW)	WF2 (kvar)	WF3 (kW)	WF3 (kvar)	FCPP1 (kW)	FCPP1 (kvar)	FCPP2 (kW)	FCPP2 (kvar)	FCPP3 (kW)	FCPP3 (kvar)	FCPP4 (kW)	FCPP4 (kvar)	FCPP5 (kW)	FCPP5 (kvar)
1	431.1	−120.21	447.48	56.43	446.57	−150.948	500.00	38.92	300.00	83.57	298.03	88.65	491.86	219.16	500.00	70.69
2	450	−85.185	446.65	82	419.42	209.637	488.64	201.20	300.00	101.53	295.90	−2.77	494.58	−150.71	500.00	194.03
3	445.98	217.94	424.04	14.77	443.71	134.262	486.89	137.14	293.72	15.41	214.96	−107.12	500.00	−149.49	481.46	7.06
4	431.01	112.93	428.02	202.51	450	−14.373	500.00	−68.21	268.89	−66.46	298.77	104.41	500.00	214.32	500.00	−150.10
5	446.94	−129.34	441.64	142.7	431.57	108.999	491.24	−67.41	295.24	−119.34	287.94	−32.87	499.85	−15.78	480.92	242.16
6	450	142.33	405.86	200.07	437.58	145.143	484.62	219.66	286.29	144.14	285.27	101.95	500.00	−35.42	476.56	−203.24
7	444.45	97.767	450	208.35	450	−101.97	484.08	−240.41	297.42	142.58	278.84	53.62	500.00	203.69	463.02	47.99
8	396.93	167.77	426.21	−27.83	430.74	204.426	474.68	128.78	281.92	−130.19	300.00	128.85	394.92	−130.54	491.28	−199.11
9	450	−107.18	353.69	−122.3	450	71.856	463.33	−75.07	280.40	111.26	262.07	90.85	500.00	−108.50	459.93	187.11
10	450	−56.66	450	180.91	418.64	127.818	448.16	108.43	300.00	98.94	275.98	117.38	500.00	40.52	468.49	−127.26
11	450	196.34	441.18	−113.6	450	102.807	490.35	218.44	291.14	6.94	210.19	−35.83	452.93	170.81	494.06	−24.23
12	448.65	171.47	425.08	139.77	445.15	65.601	453.92	114.52	299.76	30.82	290.25	−43.70	500.00	−21.76	496.27	62.28
13	450	22.635	426.82	204.02	429.61	−151.479	475.00	−214.13	298.62	118.01	278.07	35.12	445.86	−87.39	487.51	−75.29
14	422.23	189.3	413.52	183.29	363.83	177.021	500.00	57.21	291.50	−64.07	271.93	48.11	494.90	−183.11	482.51	84.18
15	430.95	217.94	443.13	−5.607	436.97	217.944	500.00	154.08	290.30	6.91	290.38	111.16	500.00	154.54	496.36	−8.10
16	440.44	214.93	450	−217.9	449.33	−203.229	481.34	197.43	293.03	−125.30	300.00	144.97	493.15	195.38	500.00	166.66
17	450	163.27	445.02	217.94	450	−107.577	500.00	186.02	300.00	−50.08	273.98	125.84	496.89	−230.42	466.29	−75.78
18	450	217.94	400.56	−201.5	439.25	−55.071	498.28	242.16	266.40	125.33	292.24	40.67	489.10	−239.59	450.25	−89.23
19	445.15	−70.07	449.3	214.29	450	202.941	478.91	235.99	239.91	28.87	297.47	63.27	481.40	208.41	500.00	2.80
20	450	140.6	450	112.09	419.17	−26.352	455.85	147.35	279.67	−56.03	282.40	−123.19	498.34	−86.61	500.00	−229.69
21	435.03	196.32	429.77	185.39	439.97	160.263	472.11	100.85	287.04	58.36	288.93	−61.75	497.26	10.39	458.50	−39.12
22	437.02	142.12	448	−191.3	450	−197.46	500.00	220.91	300.00	−0.38	300.00	64.71	471.49	−52.65	482.86	−228.13
23	435.51	193.41	423.71	−35.64	432.44	138.105	481.48	130.51	258.44	−60.97	283.58	−134.87	477.13	242.16	483.86	−96.45
24	415.26	188.44	447.75	−36.6	449.58	−79.209	499.17	−15.08	259.06	−72.59	260.72	33.53	500.00	−19.17	498.46	−108.85
Sum	10557	2424.87	10367	1392.01	10484	979.155	11608	2159.31	6858.77	327.29	6717.92	811.00	11679.69	148.23	11618.60	−589.61

losses and the emission follow the variation of the load demands properly.

Table 4 shows the stochastic optimal dispatch of WFs, FCPPs for the next day. FCPPs and WFs are installed at heavy loaded buses. According to Table 4, the DisCo should utilize the installed FCPP4 at bus #31 in a higher capacity than the other FCPPs installed in the network to achieve the best plan for most of the following 24 h. When using WFs, the best schedule is to utilize WF2 and WF3 in lower capacities than other WFs during the next day. Since WFs have intermittent characteristics, the best strategy for the DisCo is to supply the load, especially in highly loaded buses, with sources, which have lower uncertainty in the output power. The results show that in general, the DisCo tries to use FCPPs more than WFs due to their deterministic nature and lower generation cost.

Table 5 shows the optimal hourly dispatch of capacitors and transformers taps. Although, buses #34 and #64 are heavily loaded, DisCo's best strategy is not to use the installed capacitors (C4, C5) in the mentioned buses for most of the time in the next day. DisCo should try to compensate the reactive power at bus #34 using capacitor C5 more than capacitor C4 at bus #64. Capacitors C3 and C6 are utilized at a higher rate than C4, C5 while they are installed at low loaded buses #34 and #64. Generally, capacitors C3 to C6 track the load changes, when capacitors C1, C2 cannot follow these variations during the next day. Moreover, C1 and C2 are installed at infeed buses and they participate more in controlling DisCo power factor within the specified range.

In order to show that all constraints are satisfied under the proposed optimization method, the stochastic values of the voltages throughout the feeders for both light and heavy loaded hours (9 am and 9 pm) are shown in Fig. 7. In addition, Fig. 8 demonstrates the standard deviation (SD) of the voltage profile throughout the feeder for the two mentioned hours. It can be observed from Fig. 7 that the bus voltages are maintained within the permitted range of tolerance, i.e. ±5% of the nominal value by using the probabilistic multi-objective approach. Furthermore, it is evident from Fig. 8 that the standard deviation in the heavy loaded hour (9 pm) is more than the light hour, (9 am). In fact, the standard deviation of voltages increase as the hourly load demand is increased.

Table 5
Daily optimal dispatches of capacitors and transformers with DGs.

Hour	Tap1	Tap2	C1 (kvar)	C2 (kvar)	C3 (kvar)	C4 (kvar)	C5 (kvar)	C6 (kvar)
1	1.04	1.04	600	500	100	0	0	200
2	1.04	1.04	200	400	100	200	200	100
3	1.04	1.04	0	0	200	0	200	300
4	1.04	1.04	300	200	100	100	200	400
5	1.04	1.04	500	0	100	0	200	0
6	1.04	1.04	600	0	200	0	300	0
7	1.04	1.04	200	200	200	0	400	0
8	1.04	1.04	200	0	300	200	400	400
9	1.04	1.04	400	100	300	500	200	400
10	1.04	1.04	200	400	400	300	200	500
11	1.04	1.04	600	100	500	400	400	500
12	1.04	1.04	600	300	500	300	300	500
13	1.04	1.04	500	0	400	100	400	300
14	1.04	1.04	400	500	400	200	0	500
15	1.04	1.04	200	600	200	100	200	300
16	1.04	1.04	400	100	400	400	0	400
17	1.04	1.04	0	200	200	200	500	500
18	1.04	1.04	0	0	500	300	500	300
19	1.04	1.04	600	100	400	400	400	300
20	1.04	1.04	300	400	500	400	300	500
21	1.04	1.04	100	300	500	400	400	500
22	1.04	1.04	100	500	500	400	500	500
23	1.04	1.04	200	0	200	200	300	500
24	1.04	1.04	300	500	200	200	300	0

(Tap1 and Tap2 are the tap positions of LTC transformers)

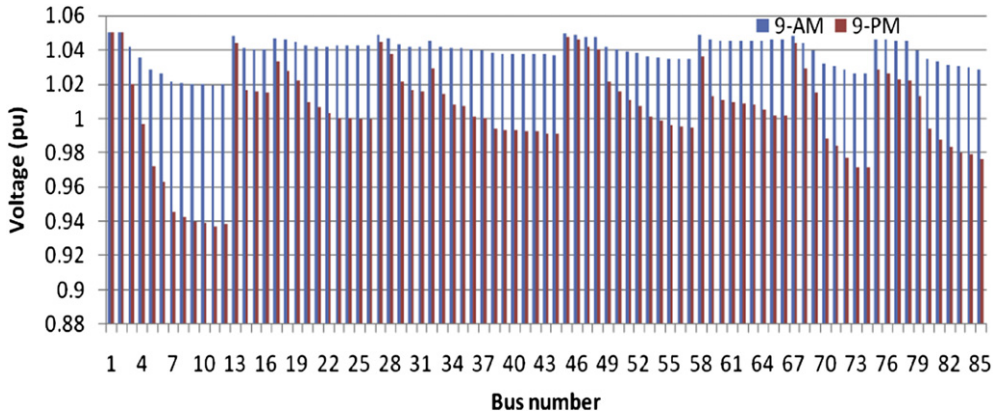

Fig. 7. Stochastic voltage profile throughout the feeder for both light and heavy loaded hours, 9 am and 9 pm.

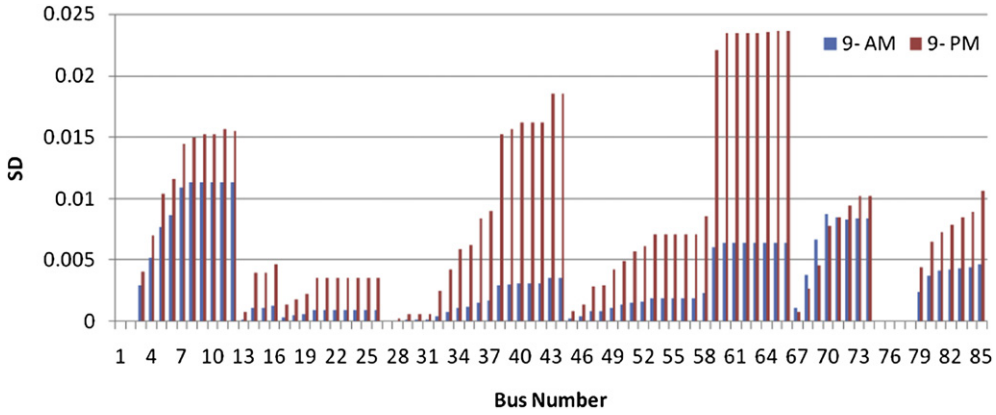

Fig. 8. Standard deviation of voltage profile throughout the feeder for both light and heavy loaded hours, 9 am and 9 pm.

In order to consider the effect of uncertainties of the load/generation on the feeders' voltage profile, the standard deviation of the voltage for some buses in the substations 1 and 2 are selected and shown in Figs. 9 and 10. As shown, SD in the buses with WFs is the largest while SD in deterministic buses is the smallest. However, the value of SDs in buses with discrete distribution load increases dramatically as the load demand increases.

The probability density function of the voltage at 9 am for buses # 51, # 58, # 77, # 79 is shown in Fig. 11. It is clear that the proposed method effectively maintains the value of voltages within the permitted range.

Although WFs are emission-free resources, they introduce more uncertainty than load values in planning the best strategy of DisCo for the next day. In fact, FCPPs produce emission, but they do not introduce uncertainty in distribution systems and are more reliable to be used by DisCos. The simulation results show that the combination of WFs and FCPPs can effectively improve the performance of the system.

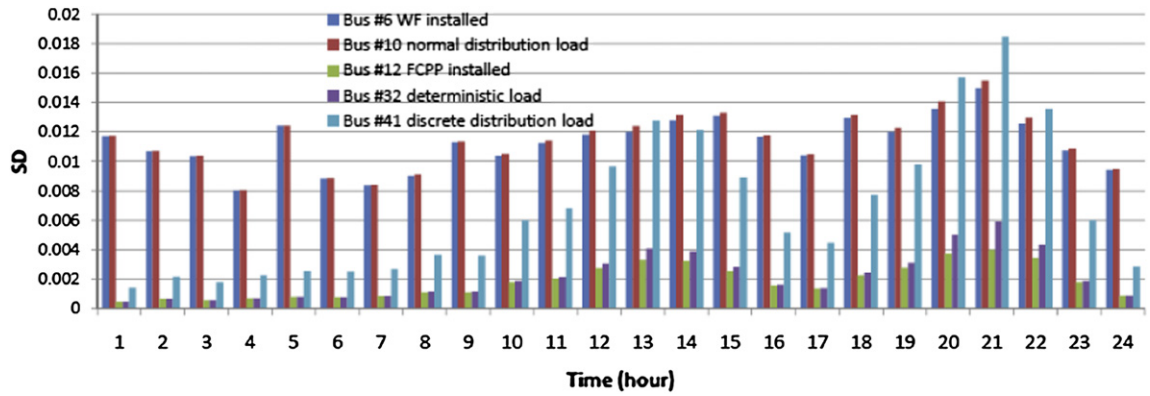

Fig. 9. Standard deviation of voltages for some buses in substation 1.

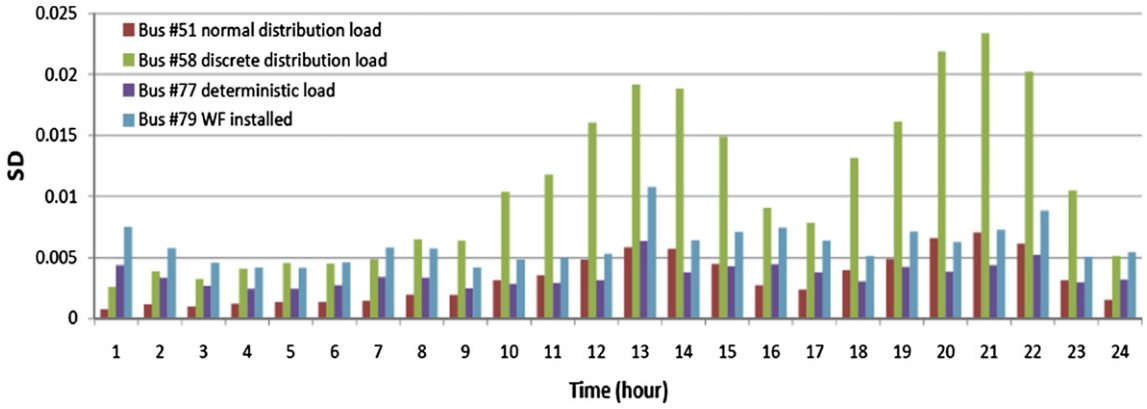

Fig. 10. Standard deviation of voltages for some buses in substation 2.

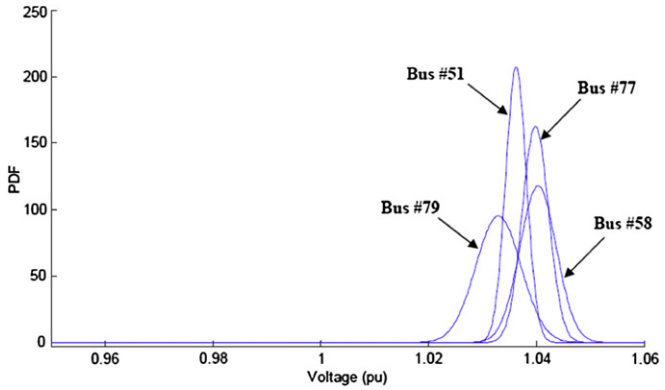

Fig. 11. Probability density function of voltages at 9 am for buses # 51, # 58, # 77, # 79.

9. Conclusion

This paper presented a new probabilistic multi-objective approach for the daily Volt/Var control in distribution systems regarding the hybrid use of fuel cell and wind energy sources. The uncertainty in the load demands and the electrical power generated by WFs was taken into account. Point Estimate Method (PEM) was used as an effective probabilistic power flow method to deal with the random behavior of WFs and load demands simultaneously. The cost of generating electrical energy, electrical energy losses, and the total emission were included in the objective function. The multi-objective optimization problem was solved using fuzzy optimization method with the max-min operator. A new optimization algorithm based on Improved Shuffled Frog Leaping Algorithm (ISFLA) was proposed to determine the DisCo's strategy, which is optimal from economical, operational, and environmental perspectives. A practical 85 bus distribution system was used to show the effectiveness of the methodology under light and heavy loaded hours. The simulation results show that the voltage magnitude of buses and substation power factors are in the desired limits. Moreover, the proposed optimization method is very precise and can be used in practical systems. Also, DisCos relying on wind farms for power generation can benefit from this study.

References

[1] Bourouni K, Ben M'Barek T, Al Taee A. Design and optimization of desalination reverse osmosis plants driven by renewable energies using genetic algorithms. Renewable Energy 2011;36(3):936–50.
[2] Niknam T, Zeinoddini Meymand H, Nayeripour M. A practical algorithm for optimal operation management of distribution network including fuel cell power plants. Renewable Energy 2010;35:1696–714.
[3] Snyder B, Kaiser MJ. Ecological and economic cost-benefit analysis of offshore wind energy. Renewable Energy 2009;34(6):1567–78.
[4] Baron ME, Hsu MY. Volt/var control at distribution substations. IEEE Transaction on Power Systems Feb. 1999;14(1):312–8.
[5] Niknam T. A new approach based on Ant colony optimization for daily volt/var control in distribution networks considering distributed generators. Energy Conversion and Management 2008;49:3417–24.
[6] Niknam T. An efficient optimization algorithm based on ACO for daily volt/var control in distribution networks considering DER. Journal of Intelligent and Fuzzy Systems 2008;20:119–32.
[7] Niknam T, Ranjbar AM, Shirani AR. A new approach based on Ant algorithm for volt/var control in distribution network considering distributed generation. Iranian Journal of Science & Technology, Transaction B 2005; 29:1–15.
[8] Niknam T, Ranjbar AM, Shirani AR. An approach for volt/var control in distribution network with distributed generation. International Journal of Science and Technology, Scientia Iranica 2005;12:34–42.
[9] Niknam T, Bahman Firouzi B, Ostadi A. A new fuzzy adaptive particle swarm optimization for daily volt/var control in distribution networks considering distributed generators. Applied Energy 2010;87:1919–28.
[10] Carvalho PMS, Correia PF, Ferreira LAFM. Distributed reactive power generation control for voltage rise mitigation in distribution networks. IEEE Transaction on Power Systems 2008;23:766–72.
[11] Madureira AG, Lopes JAP. Coordinated voltage support in distribution networks with distributed generation and microgrids. IET Renewable Power Generation 2009;3:439–54.
[12] Viawan FA, Karlsson D. Voltage and reactive power control in systems with synchronous Machine-based distributed generation. IEEE Transaction on Power Delivery 2008;23:1079–87.
[13] Su CL. Comparative analysis of voltage control strategies in distribution networks with distributed generation. IEEE/PES General Meeting; 2009:1–7.
[14] Senjyu T, Miyazato Y, Yona A, Urasaki N, Funabashi T. Optimal distribution voltage control and coordination with distributed generation. IEEE Transaction on Power Delivery 2008;23:1236–42.
[15] J. Hethey, S. Leweson, Probabilistic Analysis of Reactive Power Control Strategies for Wind Farms, Master thesis, Technical University of Denmark, 2008.
[16] P. Chen, Z. Chen, B. Bak-Jensen, R. Villafáfila, S. Sörensen, Study of power fluctuation from Dispersed generations and loads and its impact on a distribution network through a probabilistic approach, Proceeding of 9th International conference on electric power quality and utilization. Barcelona, 9–11, October 2007.
[17] Morales JM, Perez-Ruiz J. Point estimate schemes to solve the probabilistic power flow. IEEE Transaction on Power Systems 2007;22:1594–601.
[18] Hatziargyriou ND, Karatsanis TS. Distribution system voltage and reactive power control based on probabilistic load flow analysis. IEE Proceedings Generation Transmission Distribution July. 1997;144:363–9.
[19] Hatziargyriou ND, Karakatsanis TS, Lorentzou MI. Voltage control settings to increase wind power based on probabilistic load flow. Electrical Power and Energy Systems 2005;27:656–61.
[20] Bie Z, LI G, Liu H, WANG X, WANG X. Studies on voltage fluctuation in the integration of wind power plants using probabilistic load flow. Proceedings IEEE/PES General Meeting; 2008:1–7.
[21] Hong YY, Luo YF. Optimal VAR control considering wind farms using probabilistic load-flow and gray-based genetic algorithms. IEEE Transaction on Power Delivery July 2009;24:1441–9.
[22] Su C. Stochastic evaluation of voltages in distribution networks with distributed generation using Detailed distribution operation models. IEEE Transaction on Power Systems May 2010;25:786–95.
[23] Elbeltagi E, Hegazy T, Grierson D. Comparison among five evolutionary-based optimization algorithms. Advanced Engineering Informatics 2005;19:43–53.

[24] Morales JM, Baringo L, Conejo AJ, Mĩnguez R. Probabilistic power flow with correlated wind sources. IET Generation Transmission Distribution 2010;4: 641–51.
[25] Marwali MKC, Ma H, Shahidehpour SM, Abdul-Rahman KH. Short-term generation scheduling in photovoltaic- utility grid with battery storage. IEEE Transactions on Power Systems 1998;13:1057–62.
[26] Shen M, Meuleman W, Scott K. The characteristics of power generation of static state fuel cells. Journal of Power Sources 2003;115:203–9.
[27] Rosenblueth E. Point estimate for probability moments. Proceedings of National Academy of Science of United States of America 1975;72:3812–4.
[28] Hong HP. An efficient point estimate method for probabilistic analysis. Reliability Engineering and System Safety 1998;59:261–7.
[29] Su C. Probabilistic load-flow computation using point estimate method. IEEE Transaction on Power Systems November 2005;20:1842–51.
[30] Caramia P, Carpinelli G, Varilone P. Point estimate schemes for probabilistic three phase load flow. Electric Power Systems Research 2010;80:168–75.
[31] Zhang P, Lee ST. Probabilistic load flow computation using the method of combined cumulants and Gram-Charlier expansion. IEEE Transaction on Power Systems Feb 2004;19:676–82.
[32] Li G, Zhang X. Comparison between two probabilistic load flow methods for reliability assessment. IEEE Power & Energy Society General Meeting; 2009:1–7.
[33] Niknam T, Olamaie J, Khorshidi R. A hybrid algorithm based on HBMO and fuzzy set for multi-objective distribution feeder reconfiguration. World Applied Sciences Journal 2008;4:308–15.
[34] Eusuff M, . Lansey K. Optimization of water distribution network design using the shuffled frog leaping algorithm. Journal of Water Resources Planning and Management 2003;129:10–25.
[35] Eusuff M, Lansey K, Pasha F. Shuffled frog-leaping algorithm: a memetic meta-heuristic for discrete optimization. Engineering Optimization 2006;38: 129–54.
[36] Rahimi-Vahed A, Mirzaei AH. A hybrid multi-objective shuffled frog-leaping algorithm for a mixed-model assembly line sequencing problem. Computers & Industrial Engineering 2007;53:642–66.
[37] Amiri B, Fathian M, Maroosi A. Application of shuffled frog-leaping algorithm on clustering. International Journal of Advanced Manufacturing Technology 2009;45:199–209.
[38] Rahimi-Vahed A, Dangchi M, Rafiei H, Salimi E. A novel hybrid multi-objective shuffled frog-leaping algorithm for a bi-criteria permutation flow shop scheduling problem. International Journal of Advanced Manufacturing Technology 2009;41:1227–39.
[39] Chung G, Lansey K. Application of the shuffled frog leaping algorithm for the optimization of a general large-scale water supply system. Water Resources Management 2009;23:797–823.
[40] Ahuja A, Das S, Pahwa A. An AIS-ACO hybrid approach for multi-objective distribution system reconfiguration. IEEE Transactions on Power Systems 2007;22(3):1101–11.
[41] K. A. Denise, D'. Arnaud, Optimization of renewable energy resources (RERs) for Enhancing network performance for distribution systems, Master thesis, Howard University, 2010.